Electronic Supplementary Material (ESI) for Nanoscale.

Supporting Information

In-situ Etching Assisted Synthesis of Pt-Fe-Mn Ternary Alloys with High-index Facets as Efficient Catalysts for Electro-oxidation Reactions

Congli Qin,[a] Aixin Fan,[a] Xin Zhang,[a,] * Xiaoping Dai,[a] Hui Sun,[a] Danhua Ren,[a] Zhun Dong,[a] Yao Wang,[a] Chenglong Luan,[a] Jin-Yu Ye,[b] Shi-Gang Sun[b]

Table S1. The theoretical relationship between interfacial angles and facets for a concave cube.

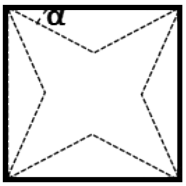

{hk0}	α (°)	{hk0}	α (°)
{810}	7.1	{520}	21.8
{710}	8.1	{730}	23.2
{610}	9.5	{210}	26.6
{510}	11.3	{740}	29.7
{410}	14.0	{320}	33.7
{720}	15.9	{430}	36.9
{310}	18.4	{540}	38.7
{830}	20.6	{110}	45.0

Miller index is always used to describe crystal plane. The angle θ between two crystals ($h_1k_1l_1$) and ($h_2k_2l_2$) is: $\theta = \arccos\left(\frac{h_1h_2 + k_1k_2 + l_1l_2}{\sqrt{\left(h_1^2 + k_1^2 + l_1^2\right)\left(h_2^2 + k_2^2 + l_2^2\right)}}\right)$.

When the z-axis intercept is infinite, the crystal planes are written (hk0). The angle α between (hk0) and (100) can be calculated by: $\alpha = \arccos\left(\frac{h}{\sqrt{(h^2 + k^2)}}\right)$.

The integers are usually written in lowest terms, so we can obtained h and k via the angle α.[1]

Table S2. Mass fraction of Pt, Fe and Mn in Pt-Fe-Mn CNC and Pt-Fe-Mn UCNC measured by ICP-OES.

	Pt-Fe-Mn CNC	Pt-Fe-Mn UCNC
Pt (wt %)	93.25	92.0
Fe (wt %)	6.03	7.40
Mn (wt %)	0.72	0.55

Table S3. Mass fraction of Pt, Fe and Mn in Pt-Fe-Mn UCNC at different reaction period measured by ICP-OES.

Sample	Pt-Fe-Mn UCNC (mass ratio) Determined by ICP-OES
2h	77.9 : 21.4 : 0.77
4h	85.9 : 13.2 : 0.85
6h	92.0 : 7.4 : 0.55
8h	93.3 : 5.88 : 0.82

Table S4. Comparison of FAOR performance of Pt-Fe-Mn NCs with other Pt-based alloyed enclosed by HIFs in acidic electrolytes available in literature

Sample	Electrolyte	Specific activity ($mA\ cm^{-2}$)	Mass activity ($A\ mg_{Pt}^{-1}$)	References
Pt-Fe-Mn CNC	0.5 M H_2SO_4 + 0.25 M HCOOH	0.83	0.071	This work
Pt-Fe-Mn UCNC	0.5 M H_2SO_4 + 0.25 M HCOOH	3.49	0.36	This work
Pt CNC	0.5 M H_2SO_4 + 0.25 M HCOOH	0.51	_	This work
Pt-Mn CNC	0.5 M H_2SO_4 + 0.25 M HCOOH	0.71	_	This work
Pt-Mn-Cu ramiform polyhedron	0.5 M H_2SO_4 + 0.25 M HCOOH	2.7	0.33	4
Pt-Ni hexoctahedral	0.5 M H_2SO_4 + 0.25 M HCOOH	0.13	0.07	5
Pt-Ni-Cu CNC	0.5 M H_2SO_4 + 0.25 M HCOOH	1.5	0.07	6
Pt_3Co deeply excavated	0.5 M H_2SO_4 + 0.25 M HCOOH	2.9	0.72	7

nanocubes				
Pt-Cu concave octahedron	0.5 M H_2SO_4 + 0.25 M HCOOH	0.96	_	8
PtAgCu@Pt Cu concave octahedron	0.5 M H_2SO_4 + 0.5 M HCOOH	1.65	0.31	9
Pt_3Sn CNC	0.1 M $HClO_4$ + 1 M HCOOH	5.00	0.65	10

Table S5. Peak Potential and Onset Potential of CO Oxidation of commercial Pt blak, Pt/C, Pt-Fe-Mn CNC and UCNC NCs.

sample	peak potential of CO oxidation (V)	onset potential of CO oxidation (V)
Pt black	0.47	0.63
Pt/C	0.51	0.59
CNC Pt-Fe-Mn NCs	0.45	0.58
UCNC Pt-Fe-Mn NCs	0.33	0.52

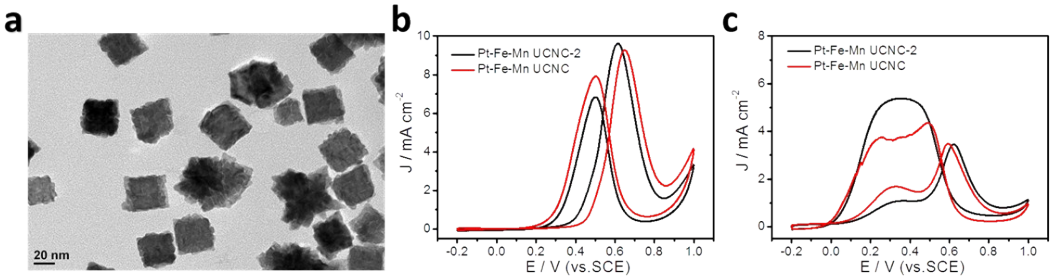

Figure S1. (a) TEM of Pt-Fe-Mn UCNC-2 CNs, (b) CV of MOR in a mixture of 0.5 M H_2SO_4 + 2 M CH_3OH at a scan rate of 50 mV s^{-1}, (c) CV of FAOR in a mixture of 0.5 M H_2SO_4 + 0.25 M HCOOH at a scan rate of 50 mV s^{-1}.

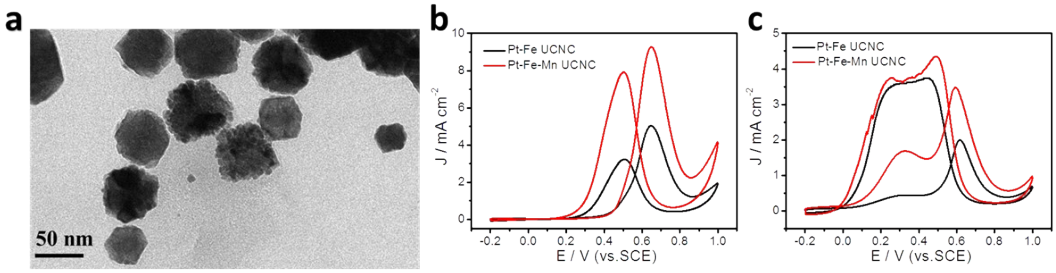

Figure S2. (a) TEM of Pt-Fe CNC CNs, (b) CV of MOR in a mixture of 0.5 M H_2SO_4 + 2 M CH_3OH at a scan rate of 50 mV s^{-1}, (c) CV of FAOR in a mixture of 0.5 M H_2SO_4 + 0.25 M HCOOH at a scan rate of 50 mV s^{-1}.

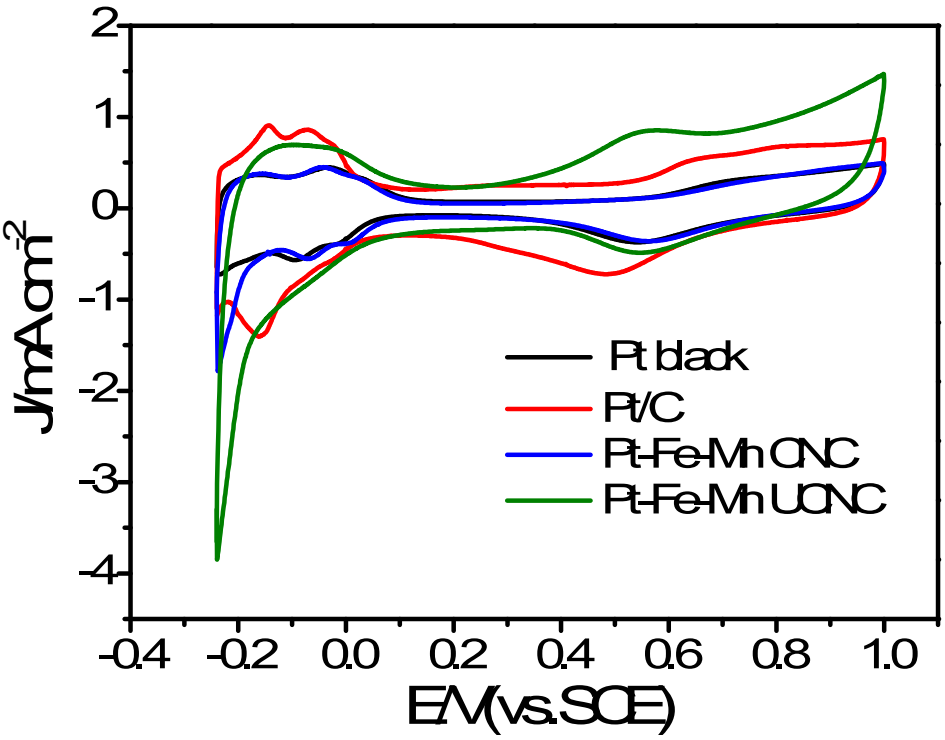

Figure S3. CV curves of the Pt-Fe-Mn CNC, UCNC NCs, Pt black, Pt/C in a N_2-Purged 0.5 M H_2SO_4 solution at a scan rate of 50 mV s^{-1}.

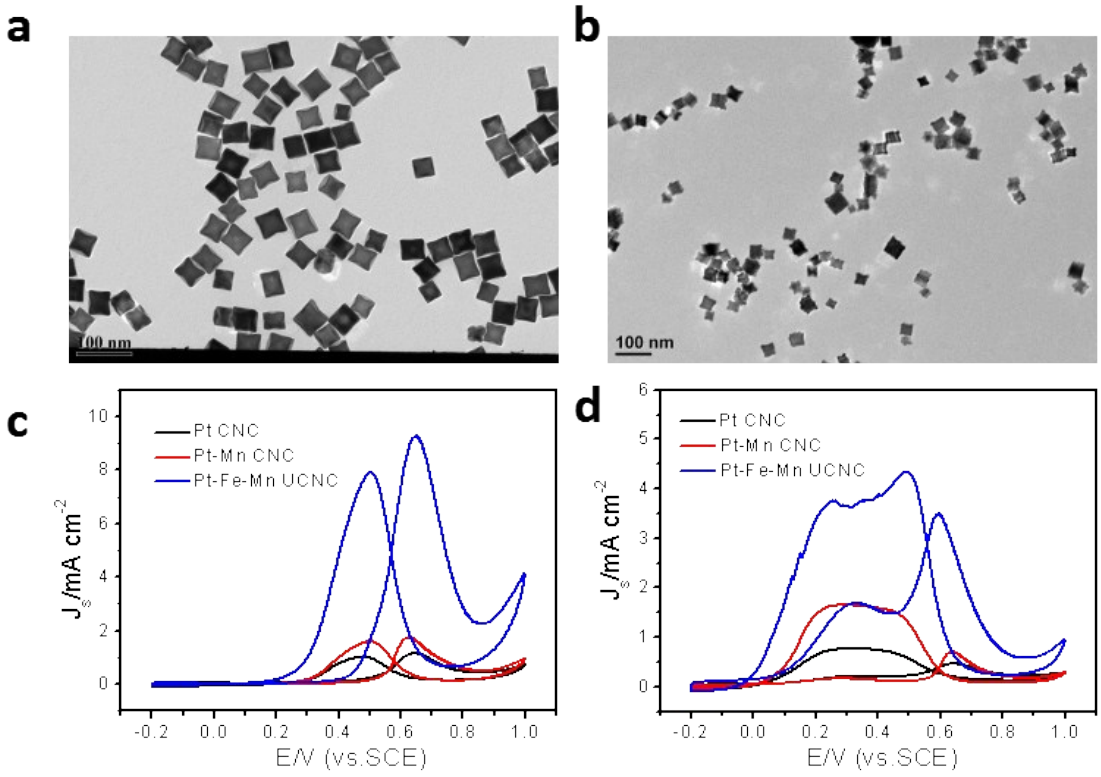

Figure S4. (a) TEM of Pt CNC CNs, (b) TEM of Pt-Mn CNC CNs, (c) CV of MOR in a mixture of 0.5 M H_2SO_4 + 2 M CH_3OH at a scan rate of 50 mV s^{-1}, (d) CV of FAOR in a mixture of 0.5 M H_2SO_4 + 0.25 M HCOOH at a scan rate of 50 mV s^{-1}. Pt CNC and Pt-Mn CNC CNs were prepared as our previous reports.[2-3]

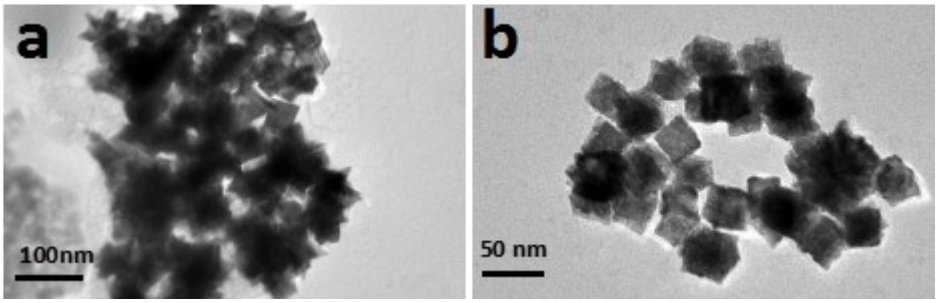

Figure S5. TEM images of the Pt-Fe-Mn (a) CNC and (b) UCNC NCs after the i-t test.

References

[1] Rong, H.; Mao, J.; Xin, P.; He, D.; Chen, Y.; Wang, D.; Niu, Z.; Wu, Y.; Li, Y. *Adv. Mater*. **2016**, *28*, 2540-2546.

[2] Zhang, Z. C.; Hui, J. F.; Liu, Z. C.; Zhang, X.; Zhuang, J.; Wang, X. *Langmuir* **2012**, *28*, 14845-14848.

[3] Wang, Y.; Zhuo, H.; Zhang, X.; Dai, X.; Yu, K.; Luan, C.; Lei, Y.; Xiao, Y.; Li, J.; Wang, M.; Gao, F. *Nano Energy* **2018,** *48*, 590-599.

[4] Luan, C.; Zhou, Q. X.; Wang, Y.; Xiao, Y.; Dai, X.; Huang, X. L.; Zhang, X. *Small* **2017**, *13*, 1702617.

[5] Xu, X.; Zhang, X.; Sun, H.; Yang, Y.; Dai, X.; Gao, J.; Li, X.; Zhang, P.; Wang, H. H.; Yu N. F.; Sun, S. G. *Angew. Chem., Int. Ed*. **2014**, *53*, 12522-12527.

[6] Zhang, P.; Dai, X.; Zhang, X.; Chen, Z.; Yang, Y.; Sun, H.; Wang, X.; Wang, H.; Wang, M.; Su, H.; Li, D.; Li, X.; Qin, Y. *Chem. Mater*. **2015**, *27*, 6402-6410.

[7] Du, H.; Luo, S.; Wang, K.; Tang, M.; Sriphathoorat, R.; Jin, Y.; Shen, P. K. *Chem. Mater*. **2017**, *29*, 9613-9617.

[8] Gao, D.; Li, S.; Song, G.; Zha, P.; Li, C.; Wei, Q.; Lv, Y.; Chen, G. *Nano Research* **2018**, *11*, 2612-2624.

[9] Fu, G. T.; Xia, B. Y.; Ma, R. G.; Chen, Y.; Tang, Y. W.; Lee, J. M. *Nano Energy* **2015**, *12*, 824-832.

[10] Rong, H.; Mao, J.; Xin, P.; He, D.; Chen, Y.; Wang, D.; Niu, Z.; Wu, Y.; Li, Y. *Adv. Mater*. **2016**, *28*, 2540-2546.